TWENTY FIRST EUROPEAN ROTORCRAFT FORUM

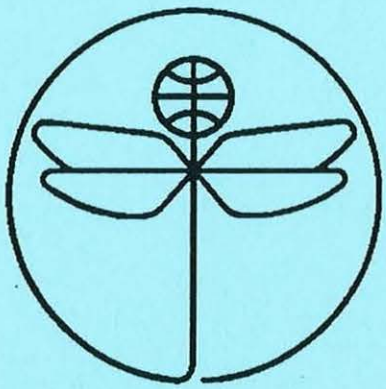

Paper No II.2

AERODYNAMIC MOMENTS ON ROTOR BLADES IN FORWARD FLIGHT: TEST RESULTS AND MODELING

BY

Jean-Joël Costes

ONERA
FRANCE

August 30 - September 1, 1995

SAINT - PETERSBURG, RUSSIA

Paper nr.: II.2

Aerodynamic Moments on Rotor Blades in Forward Flight: Test Results and Modeling.

J.-J. Costes

TWENTY FIRST EUROPEAN ROTORCRAFT FORUM
August 30 - September 1, 1995 Saint-Petersburg, Russia

AERODYNAMIC MOMENTS ON ROTOR BLADES IN FORWARD FLIGHT: TEST RESULTS AND MODELLING

Jean-Joël Costes
ONERA
BP 72 - 92322 France

Abstract

An analysis is made of experimental data concerning aerodynamic moments on a rotor blade in forward flight at high advance ratios. Two phenomena are not predicted by standard codes: the large nose up moment at the blade tip around the 0° azimuth angle and the strong nose down moment around the 90° azimuth angle for inboard sections. A tentative explanation is made of the physical phenomena and a corrective extension is made to a standard 2D model.

1. Introduction

In 1991 a comprehensive set of experiments was conducted in the S1 wind tunnel in Modane (France) on a helicopter rotor with rectangular blade tips (4.2m diameter). Unsteady aerodynamic forces were measured using pressure transducers at five blade sections (figure 1) at the following spanwise positions: r/R_1 = 0.975, 0.915, 0.825, 0.700 and 0.500 (where R_1 is the radius of the rotor disc). The blade flap, lead-lag and pitching rigid body motions were measured by means of angular displacement sensors located at the hinges. The bending and torsional components of the blade deformations were obtained from the responses of strain gauges on a specially instrumented blade using the strain pattern analysis technique [5]. Thus the absolute movement of the five instrumented blade sections is known, though with an undetermined level of accuracy.

In this paper, comparisons are presented between measured and computed aerodynamic forces. From the point of view of the aerodynamicist, the aerodynamic theories may be separated in two broad classes: those which are entirely 3-D and are able to describe the flow field around the blade, both spanwise and chordwise (full potential, Euler and Navier-Stokes codes), and those which are only partially 3-D and intrinsically make use of the 2-D notion of angle of attack (doublets or vortices lifting line(s), induced velocities, actuator disc, dynamic inflow...). The latter theories are used in the design of helicopter rotors when a great number of independent computations is necessary. This is of course the case when the aeroelastic behaviour of the rotor blades is taken into account. These simplified theories are the subject of this paper where the main objective is to improve the prediction of the aerodynamic moments on rotor blades.

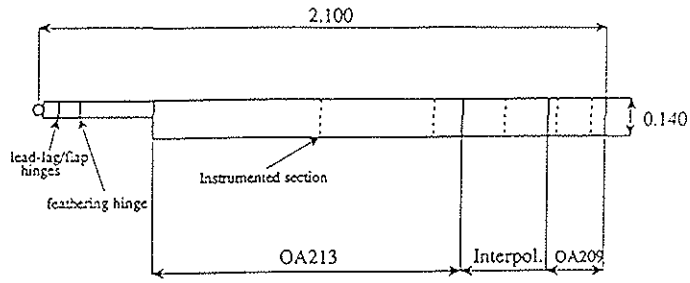

Figure 1. Schematic drawing of the rotor blade

2. Calculation of 2-D aerodynamic forces on a profile

Over the past decade a semi-empirical mathematical model (EDLIN) has been developed at ONERA [2] to synthesise 2-D experimental data on helicopter blade profiles. This model is standard for aeroelastic computations on helicopter rotors at ONERA and is fairly widely used by other establishments. The model can be used for lift, moment and drag forces on heavily loaded blades with stall on the retreating side of the rotor disc. In the present paper stall is not an issue and computations are restricted to flight cases with moderate lift.

2.1. Modelling the forces with differential equations

A comprehensive presentation of the model can be found in references [2] and [3]. For the sake of clarity the part of the model covering cases without stall is detailed here. Though the cases discussed in this paper are limited to this condition, all the numerical calculations were carried out with the complete ONERA model.

2.1.1. Modelling of the lift forces The aerodynamic lift force on a profile with chord $c = 2b$, placed at an angle of attack Θ in a wind tunnel, with ρ the density of the air and V the upstream velocity, is given by:

$$F = \frac{1}{2}\rho S\left[sb\frac{dw_0}{dt} + kb\frac{dw_1}{dt} + V\Gamma_1\right] \qquad (1)$$

$$\frac{d\Gamma_1}{dt} + \frac{\lambda V}{b}\Gamma_1 = \frac{\lambda V}{b}\frac{\partial C_{zL}}{\partial\Theta}W_0 + \sigma\frac{\lambda V}{b}W_1 + \alpha\frac{\partial C_{zL}}{\partial\Theta}\frac{dW_0}{dt} + \alpha\sigma\frac{dW_1}{dt}$$

where:

- F is the lift force and S is a reference surface: S = c × 1 metre
- λ, α, s, σ, k are coefficients which depend only on the Mach number and thus vary with time;
- C_{zL} is the steady lift coefficient when the angle of attack is moderate;
- W_0 and W_1 are components of the velocity induced by the profile and measured in the direction normal to the free stream velocity.

If x is the distance measured in the chordwise direction along the profile from the leading edge to the quarter chord axis, then the component $W(x,t)$ is given by:

$$W(x,t) = W_0(t) + xW_1(t)$$

For a profile with pitch and plunge motions:

$$W_0 = V\Theta - \frac{dh}{dt} \qquad W_1 = b\frac{d\Theta}{dt}$$

where dh/dt is the plunge velocity.

Equations (1) show that W_0 and W_1 are inputs given by the profile movement (pitch and plunge) and that the complete calculation of the lift force F is possible only after determining Γ_1 which is a circulation defined by a differential equation. The initial condition for Γ_1 in this differential equation is unknown and must be determined with the additional condition that it is periodic when W_0, W_1 and Θ are periodic functions of time.

2.1.2. Modelling of the moment around the quarter chord axis When there is no stall, the moment of the aerodynamic forces is given by formulae simpler than those for lift :

$$M_f = \frac{1}{2}\rho Sc\left[V^2C_{Mf}(W_0/V) + \Gamma_1\right] \qquad (2)$$

$$\Gamma_1 = \bar{\sigma}b\frac{dW_0}{dt} + \sigma VW_1 + sb\frac{dW_1}{dt}$$

where:

- M_f is the moment of the aerodynamic forces around the fore quarter chord axis;
- s, σ and $\bar{\sigma}$ are coefficients which depend only on the Mach number and take different values from the ones used in equations (1). This is also true for Γ_1
- C_{Mf} is the moment coefficient measured with steady state conditions and a moderate angle of attack (no stall).

Comment 1: When the velocity V is equal to 0 and Θ and h still vary with time, then $V^2C_{Mf} = 0$ and Γ_1 is bounded so that M_f (the aerodynamic moment) remains finite.

Comment 2: The model for the moment (equations 2) is much simpler than the model for the lift (equations 1). There is no differential equation. The term Γ_1 is completely determined by the velocity of the fluid, the profile plunge velocity and the profile first and second time derivatives of the angle of attack. When the angle of attack is large, the complete model which introduces a coefficient Γ_2 should be used:

$$M_f = \frac{1}{2}\rho Sc\left[V^2C_{Mf}(W_0/V) + \Gamma_1 + \Gamma_2\right] \qquad (3)$$

The coefficient Γ_2 is determined by a second order differential equation. The starting values of Γ_2 and of $d\Gamma_2/dt$ are unknown and must be determined by the additional condition that Γ_2 is a periodic function of the time variable.

2.2. Limitations of the model for the computation of aerodynamic forces

Most of the mathematical models in the literature, and particularly the one presented above, are based on 2D experimental results and on flat plate theory (e.g. Theodorsen, Küssner). These results are valid when the velocity of the fluid is constant at infinity upstream. This is not the case for a profile on a helicopter blade except for the hovering rotor. At high advance ratios the profile experiences a strong cyclic variation of the normal velocity and of the sweep angle. In actual fact the ONERA model has been made to agree with Greenberg's theory [6] for the lift and the same formulation has been taken by analogy for the moment. This theory includes the effect of a pulsating free stream velocity. It must be noted that for the aerodynamic moment, the extension of the ONERA model to include the rate of change of the free stream velocity is only conjectural. Even a qualitative knowledge of the effects of this rate on the aerodynamic moment is lacking.

In equations (2), when the angle of attack Θ is a constant and the plunging motion is neglected ($h = 0$), the moment is proportional to C_{Mf} and is close to zero for profiles which are weakly cambered such as those used

for helicopter blades. This conclusion can be extended to the case of small angles of attack because Γ_1 remains moderate. Thus, even with a large variation of the free stream velocity, equations (2) do not predict large moments when there is no stall. This result is in contradiction with the analysis of the experimental data for high advance ratios which shows that at the tip of the blade and in the first quadrant of the rotor disc there is a strong nose up moment followed by a strong nose down moment around the 90° blade azimuthal position [1].

The experiments carried out in Modane in 1991 confirm this finding [4] and also reveal the presence of a strong nose down moment for the inboard sections of the blade on the advancing side of the rotor disc. The presence of such large moments is entirely unexpected at this azimuth (60° to 150°) since the angle of attack remains quite moderate (less than 10°). To date, this phenomenon has been largely overlooked as it only acts on inboard blade sections and thus only moderately affects the blade torsional motion. However, this effect is not negligible when considering pitch link loads. It therefore appears necessary to complete the ONERA model (EDLIN) to account for these phenomena.

3. Selection and analysis of the experimental data

Extensive experimental data was considered covering advance ratios from 0.2 to 0.5 and moderate lift (to avoid stall). It was used to establish the extension to the ONERA classical mathematical model though in this paper only 3 cases are presented (Table 1). These were selected for their interest and comparable lift coefficients.

3.1. Computation of the angles of attack for a profile on a rotor disc

The angle of attack of a profile is one of the most important parameters needed for the computation of the aerodynamic forces. The angle of attack is essentially a 2D notion but it is a very useful engineering tool for 3D calculations even if it cannot be directly measured on a rotor blade section. Here the angles of attack are deduced from the measured lift forces.

3.1.1. Quasi steady computation of the angles of attack

For a thin profile at a moderate angle of attack α (in radians), the theoretical lift coefficient is

$$C_L = \frac{2\pi\alpha}{\sqrt{1-M^2}}$$

The Modane test data includes the forces normal to the profile in the form of the coefficient $C_N M^2$ and the lift coefficient can be deduced from:

$$C_L = \frac{C_N M^2}{M^2 \cos\alpha}$$

Combining these two formulae gives the following relation for the angle of attack (in degrees):

$$\alpha = \frac{C_N M^2}{M^2 \cos\alpha} \cdot \frac{\sqrt{1 - M^2}}{2\pi} \cdot \frac{180}{\pi} \qquad (4)$$

Though equation (4) is transcendental in α, when α is small cos α remains close to 1 and the numerical resolution of (4) is straightforward. The angles of attack computed for the five instrumented sections are shown in figure 2 for test case n°317.

One obvious question is how accurate these angles of attack are since they are computed using a quasi-steady formula ? A part of the answer can be given by looking at the effect of using quasi-steady angles of attack to compute the lift in the complete ONERA mathematical model. The results in figure 3 show that the experimental and recomputed lifts are in rather good agreement almost everywhere. This suggests that the quasi-steady angles of attack are a good measure of the actual angles on the blade profiles.

3.1.2. Unsteady computation of the angles of attack

Nevertheless, figure 3 still shows some discrepancies at the 120° azimuth angle and it is tempting to further improve the results. This may be done in the following way:

(i) the angle of attack is periodic and is supposed to contain a given number of harmonics (10 here). The coefficients of the harmonics are given (21 coefficients here). As the variation of the Mach number is known, the lift is computed by the standard ONERA model;

Table 1. Selected rotor test cases (α_D is the inclination of the rotor disc to the horizontal plane)

Test N°	Adv. ratio	α_D	Lift coef.	Lift force (N)	longitudinal force (N)
317	0.40	-8.59°	14.81	4336.0	472.4
337	0.45	-11.45°	14.18	4343.2	589.5
358	0.50	-14.11°	14.07	4281.9	731.3

(ii) a least square error is calculated and the coefficients of the angle of attack are adjusted so as to minimise the error. Any minimising algorithm can be chosen; the one used to obtain the results presented in this paper is the downhill simplex (amoeba) method of Nelder and Mead [in ref. 8]. This method is slow but particularly robust. It can also be easily modified to take into account inequalities by the penalty method.

It should be noted however that in general the unsteady angles of attack cannot be obtained with any reliability when stall appears on the retreating side of the rotor disc. This is due to the non linearities of the problem and the lack of uniqueness of the solution.

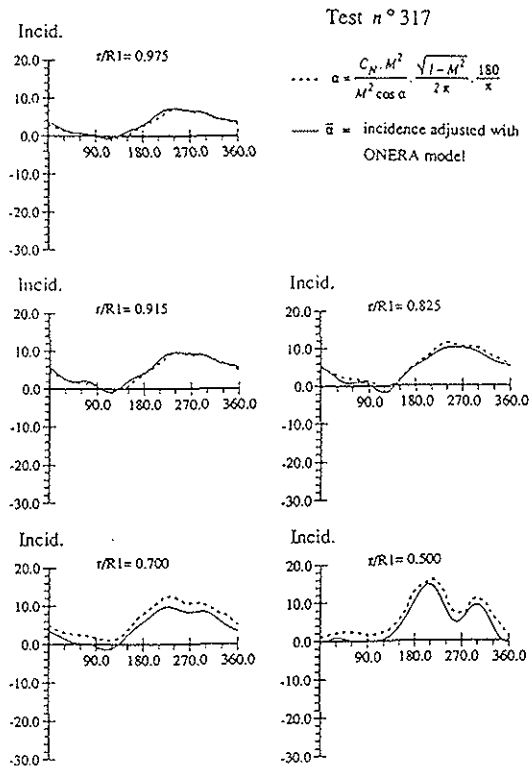

Figure 2. Comparison between angles of attack computed using a quasi-steady formula and the ONERA model (EDLIN)

For the case presented here, stall is not a problem and the quasi-steady solution is already excellent. Thus the unsteady values of the angle of attack were always obtained without difficulty. The results are shown in figure 2: steady and unsteady values are only marginally different. The virtually constant difference noticeable on the two inboard most sections (r/R_1 = 0.700 and r/R_1 = 0.500) is a consequence of the fact that for the OA213 profile lift is zero at an angle of attack of -2° instead of the usual zero degrees.

As with the quasi-steady angle of attack, the lift force is recomputed with the complete ONERA model and shows the expected improvement in the correlation between the experimental and theoretical lift forces (figure 3).

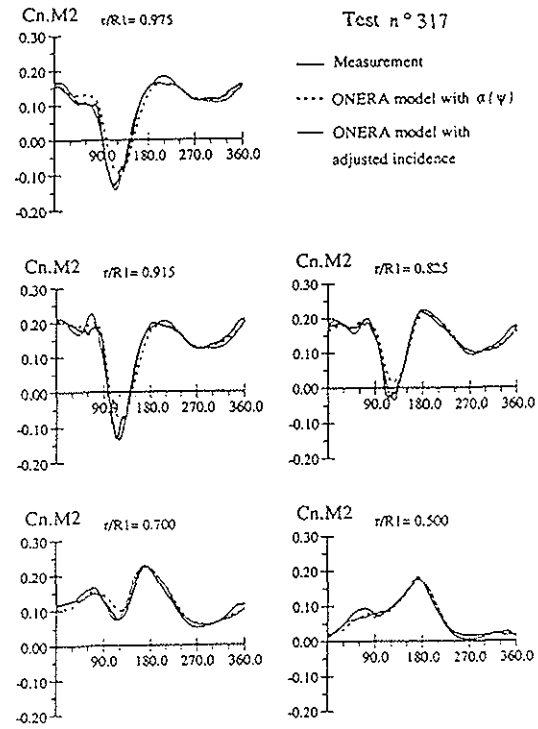

Figure 3. Lift: comparison between experiment and the ONERA model using calculated angles of attack

3.2. Aerodynamic moment about the quarter chord axis

In order to compute the aerodynamic forces and especially the moments, it is necessary to know the profile's velocity and its angle of attack. The blade speed was measured with sufficient accuracy but the angles of attack were deduced as shown in 3.1 above. These angles are model dependent, that is to say they were computed from the measured lift forces using a model, either linear quasi-steady or unsteady (ONERA). Fortunately, these computed angles of attack are not very different, thus suggesting that they represent some reality and may be a useful engineering tool even for the 3D problem of the helicopter rotor.

The quasi-steady and unsteady angles of attack can now be used to compute the aerodynamic moments around the quarter chord axis of the profile using the ONERA model. The results are shown in figure 4 in the form of the coefficient $C_M M^2$ which is proportional to the actual moment of the aerodynamic forces. The scale is the same for all five sections. As may be expected, the differences obtained between the use of the steady and the unsteady angles of attack is negligible. The comparison with the experimental results shows the previously mentioned fact that the strong nose up moments at the tip of the blade (r/R_1 = 0.975 and r/R_1 = 0.915) are not predicted. This is also the case for the large nose down moments on the advancing side of the rotor disc for the inboard sections (r/R_1 = 0.700 and r/R_1 = 0.500).

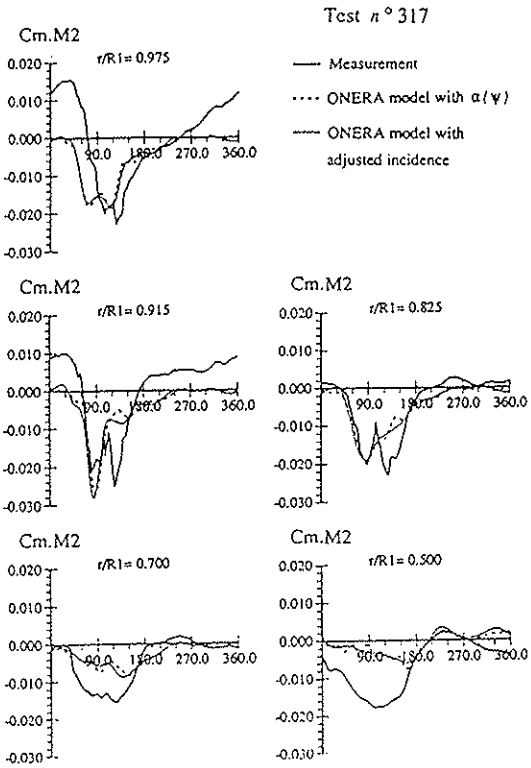

Figure 4. Moment: comparison between experiment and the ONERA model using calculated angles of attack

4. Extension to the ONERA model for moments

The standard ONERA model (EDLIN) has been thoroughly validated for cases where stall is predominant. Moreover, it is extensively used at ONERA and elsewhere and many different profiles have been modeled. It therefore seems reasonable to look for some corrective elements to apply to this existing model rather than to develop a new one from scratch. The correction which is sought must satisfy the following conditions :

- It must act only on the moment;
- It should not distinguish between an angle of attack due to a pitching or to a plunging motion. This is a consequence of the manner in which the angle of attack was deduced from the lift (see 3.1)
- It must be large for small angles of attack and small on the retreating side of the rotor disc (where the angles of attack are large !). This condition is necessary because the existing model already gives satisfactory results for the retreating blade;
- It should introduce only terms which are not already considered correctly in the standard model;
- It must be simple enough for an easy implementation into existing codes and it must not add a significant amount of computing time;
- When used in an aeroelastic code the correction must improve (and not deteriorate !) the correlation between theory and experiment.

4.1. Correction proposed for the calculation of the moments

As shown in equations (1) and (2), the lift and the moment are given by a sum of terms determined individually by differential equations. Here a similar approach is applied: a supplementary term C_{M3} is added to equation (3) thus giving :

$$M_t = \frac{1}{2}\rho Sc\left[V^2 C_{M\alpha}(W_0/V) + \Gamma_1 + \Gamma_2 + V^2 C_{M3}\right] \quad (5)$$

In this equation the C_{M3} term depends on an equivalent angle of attack Θ identified as the ratio between the components of the profile velocity at the quarter chord axis :

$$\Theta = \tan^{-1}\frac{W_0}{V}$$

Comment 1: As stated in [2] the mathematical model used for the prediction of the moments (equation (3)) tries to take into account the rate of change of the fluid velocity in the same way as for the lift forces. Nevertheless there is no theoretical or experimental basis for this modelling.

Comment 2: The angle of sweep (and its quasi-steady variation) is not entirely ignored in equations (2) and (3) because the classical model makes use of the component of the fluid velocity normal to the blade leading edge.

As may be deduced from the above comments, the modelling of the moments is only valid for profiles with pitching oscillations in steady flow. The extensions are highly conjectural and have no experimental basis. This is why the added C_{M3} term is also made to depend on the variation of the Mach number, on the angle of sweep Λ and on the rate of change of this angle. Moreover, C_{M3} is taken to be proportional to the Mach number to make it tend explicitly to zero when the velocity of the profile decreases.

4.2. Mathematical definition of the term C_{M3}

In the classical ONERA model the lift and the moment are made to depend on terms such as Γ_1 or Γ_2 which are determined by differential equations. The same approach is used here for C_{M3} which is defined by the following equation:

$$C_{M3}(\tau) = \sum_k c_k C_{M3}(\tau - k\Delta\tau) + f_3(M, \Lambda, \ldots) \quad (6)$$

Equation (6) is the discrete-time equivalent of a differential equation. In this equation the c_k terms are constant coefficients, $\Delta\tau$ is a reduced time step and f_3 is a forcing term. The reduced time step $\Delta\tau$ has been arbitrarily chosen as equal to the time taken by a particle of air to travel along a distance equal to half the chord length. The maximum number of coefficients c_k must be determined experimentally, here three terms are sufficient. The comparatively large time interval taken in (6) does not allow high frequency fluctuations of C_{M3}. A smaller $\Delta\tau$ is possible but unnecessary and would result in a greater number of coefficients c_k. Initially, the coefficients c_k were assumed to vary with the local normal Mach number but numerical tests have shown that the c_k could be made constant without any loss of accuracy in the model. This is fortunate because a very important condition for equation (6) is its stability and this can be easily checked. By stability is meant that without an external driving force ($f_3 = 0$) and for any starting values of $C_{M3}(\tau - k\Delta\tau)$, where $1 \leq k \leq 3$, the coefficient $C_{M3}(\tau)$ must converge to 0 after a finite time interval. The necessary condition for stability [8] is that the following polynomial with real coefficients has all its complex roots inside the unit circle $| Z | \leq 1$:

$$Z^N - \sum_{k=1}^{N} c_k Z^{N-k} = 0 \qquad \text{(here } N = 3\text{)}$$

There is no definite advantage in taking a discrete-time equation for C_{M3} instead of a more conventional differential equation. Both types of equation require an adjustment of the starting values in order to satisfy the periodicity condition. A discrete-time equation was chosen in this study because of the ease with which the number and the form of the coefficients c_k could be changed. A final version of the model could possibly use a differential equation for the sake of homogeneity with the EDLIN equations.

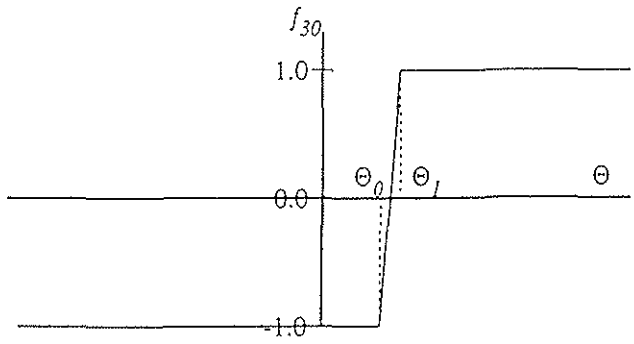

Figure 5. f_{30} as a function of Θ

4.3. Definition of the forcing term f_3

The forcing function f_3 must now be defined. As stated above, C_{M3} is made to tend to zero when the Mach number M goes to zero. This is accomplished by having f_3 given by a polynomial such as:

$$f_3 = M f_{31} + M^2 f_{32} + M^3 f_{33} + \ldots \qquad (7)$$

The functions f_{31} , f_{32} , f_{33} , ... are made to depend on the angle of sweep $\Lambda(\tau)$, on its rate of change ($\Lambda(\tau)$ - $\Lambda(\tau - \Delta\tau)$) and on the rate of change of the Mach number ($M(\tau) - M(\tau - \Delta\tau)$). A limited polynomial expansion with respect to the three new variables is used. In fact f_{31} is limited to the first and second degree and f_{32} and f_{33} to the first degree. The terms of degree zero have not been included because the classical model needs no corrections for steady conditions. No f_{3n} terms other than the first three are used.

The definition of f_3 as given by (7) is not entirely satisfactory as the influence of the angle of attack Θ has been ignored. Though the coefficient C_{M3} which is determined by f_3 is only a corrective term of the classical mathematical model, the following simple arguments show clearly that f_3 actually depends on the angle of attack.

4.3.1. Case of a symmetrical profile. Let us consider a symmetrical profile at some positive angle of attack. If some unsteady effect (variation of velocity or of the sweep angle) induces a negative moment, then, by symmetry, at a negative angle of attack, the same unsteady effect will induce a positive moment. In actual fact, some such phenomenon where the aerodynamic moment is not very dependent on the angle of attack (except for the sign) but is generated by some unsteady process, seems to act at the tip of the blade. As can be seen in figures 6, 10, 11 and 13 for the two sections closest to the tip, the moment between the 60° and 180° azimuthal positions is generally negative but there is also a sharp increase in the moment in the middle of this interval (between the 90° and the 120° azimuths). This peak has a favourable effect on the blade torsion because it corresponds to a decrease in the absolute value of the moment. The azimuthal position of this peak seems correlated with negative values of the lift force on the blade section. Thus the aerodynamic angle of attack changes from positive to negative and the large moment induced by the unsteady conditions of the flow must also change sign. Looking at the figures, it seems as if the moment tries to do exactly that but with a time delay which allows the aerodynamic angle of attack to become positive again before the moment has sufficient time to reach its expected maximum value.

This reasoning suggest a different form for the f_3 function:

$$f_3 = f_{30}\left[M f_{31} + M^2 f_{32} + M^3 f_{33}\right] \qquad (8)$$

The f_{30} function is shown in figure 5. It has values of ±1 with a linear transition between these two values. This transition takes place between the angles of attack Θ_0 and Θ_1. For a symmetrical profile $\Theta_0 + \Theta_1 = 0$ but equation (8) can also be used for a non symmetrical profile. The angles of attack Θ_0 and Θ_1 are dependent on the profile considered and on the Mach number:

$$\Theta_i = \Theta_{i0} + \Theta_{i1} M^2 \qquad i = 0 \text{ to } 1 \qquad (9)$$

The difference between Θ_0 and Θ_1 remains small for the profiles of the rotor blades (less than 3.5 degrees) over the full range of Mach numbers ($0 \leq M \leq 1$).

More complex equations for Θ_i and f_3 than those of (8) and (9) have been tried but without any significant improvement to the final results.

4.3.2. Case of a non symmetrical profile. What has been said so far concerning the forcing function f_3 is only valid for a symmetrical profile. If the profile is not symmetrical, the forcing function may not be the same for positive and negative values of the angle of attack. To cover this case, three polynomial terms are added to the function f_{31}. In these three terms the angle of attack Θ is multiplied by the sweep angle Λ and the rates of change of Λ and of the Mach number.

4.4. Numerical determination of the supplementary term C_{M3}

The mathematical definition of C_{M3} has been explained above. For each profile there are 25 parameters to determine. As shown in figure 1 the OA209 profile is used at the tip of the Modane test blade and the OA213 profile on the inner part. The blade span between these two profiles has a linearly interpolated profile. On this part of the blade span the 25 parameters are interpolated accordingly. For the complete rotor a total of 50 parameters needs to be adjusted over the whole range of advance ratios. Only the azimuthal range from 0° to 180° is considered when adjusting the parameters (using the simplex method) but the extension of the ONERA model is applied over the whole range of azimuths (0° to 360°) in obtaining the final results in figure 6.

4.5. Discussion and comments on the numerical results

Figure 6 shows that the prediction of the nose up moment around 0° azimuth is much improved and this is also the case for the large nose down moment on the inboard sections around 90° azimuth.

However, the nose down moment for the tip section between 60° and 180° azimuths, with the sharp peak in the middle of the interval, is scarcely improved, especially at the advance ratio of $\mu = 0.50$.

At this stage it is useful to get some idea of the relative importance of the different parameters involved in the corrective term C_{M3}. This can be done by putting some selected coefficients to zero and examining the effect on the moment curves. Of course the interpretation of these results can only be qualitative and is subject to personal appreciation. As it is not possible to show all the curves in the limited space of this paper, the tendencies are shown in Table 2.

This shows that the angle of attack and the rate of change of the sweep angle are not very important for the sections at the tip of the blade. The other parameters: quasi-steady sweep, rate of change of the Mach number and non linear Mach number effects are important.

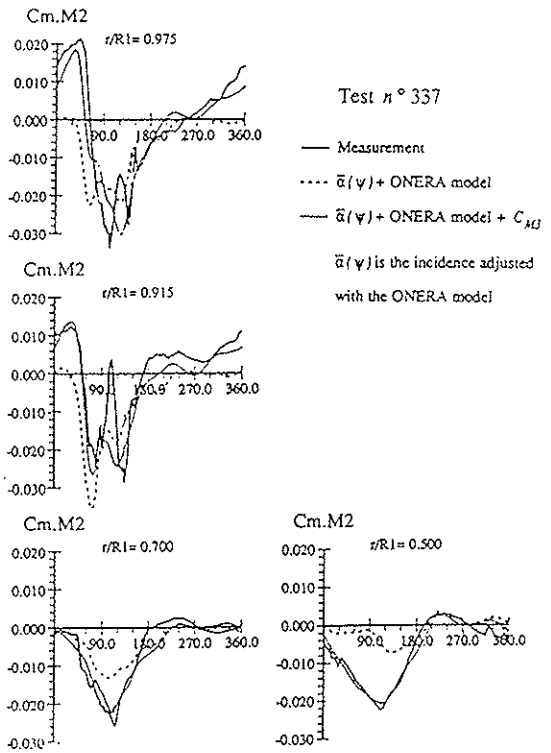

Figure 6. Moments given by the ONERA model with and without the supplementary term C_{M3}

Table 2. Influence of various parameters on the supplementary term C_{M3}

Parameter	Effect on tip sections	Effect on inboard sections
Effect of angle of attack in function f_3	*not important*	*changes the amplitude but not the shape*
$f_{32} = f_{33} = 0$	*important*	*important*
Rate of change of Mach number	*important*	*important*
Rate of change of sweep	*not important*	*important*
Sweep + sweep rate	*important*	*important*

For the inboard sections, all parameters are important but the angle of attack is perhaps less so than the others. As stated above, only the nose down moment around the 90° azimuth which is not predicted by the classical model is studied here.

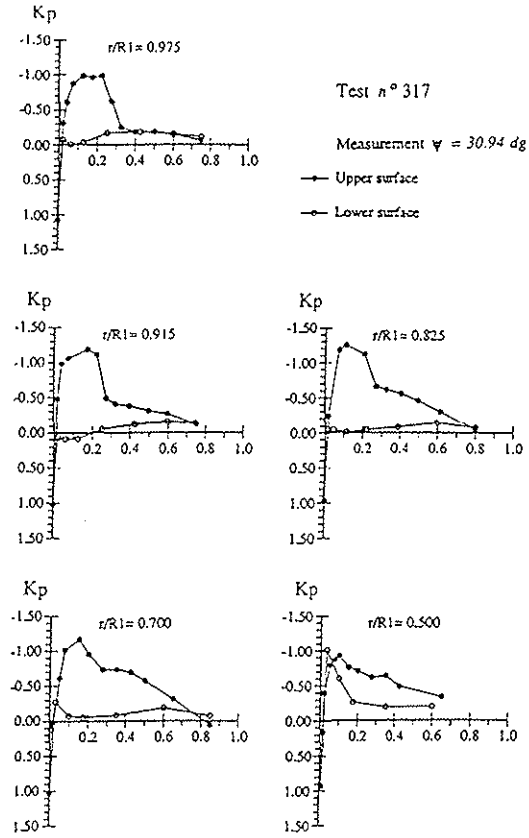

Figure 7. Measured pressure distributions for test case n°317 at 31° azimuth angle

5. Physical phenomena on advancing blades at high μ

Even if the comments in 4.5. above and in table 2 are interesting for the modelling of the aerodynamic moments, they give little idea of the physical phenomena acting on the blades. The pressure measurements recorded during tests n° 317, 337 and 358 are discussed below in order to get some insight. For each instrumented section there are n_1 unsteady pressure transducers on the upper surface and n_2 on the lower surface with $11 \leq n_1 \leq 13$ and $6 \leq n_2 \leq 8$. The numbers n_1 and n_2 depend on the section and also on the test run because the number of non functioning transducers kept increasing as the experiment progressed.

As in 4.5, the sections close to the blade tip and those at more inboard positions are commented separately.

5.1. Pressure measurements on tip sections

The pressure measurements for test n°317 at an advance ratio of $\mu = 0.40$ are given in figures 7 and 8. Figure 7 shows that shocks are already present at the tip sections at an azimuth angle of 31° and this is unexpected. The large (negative) pressures at the leading edge on the upper surface are responsible for the nose up moments recorded.

At 90° azimuth (figure 8), the shock has moved a long way towards the trailing edge and pressure is also high on the downstream side of the quarter chord line. This explains part of the strong nose down moment. The phenomenon is further reinforced by high pressures on the leading edge lower surface, a part of which is a consequence of the very small angles of attack tending to become negative.

These comments are also valid for test cases 337 and 358 except that shocks are already present at 0° azimuth. The pressure measurements make it clear that unsteady transonic phenomena are acting at the blade tip on the advancing side of the rotor disc as early as 0° or 30° azimuth angles. Tip vortex or other viscous effects do not seems to play a significant role. This conclusion is further reinforced by calculations published in [4] and [7] from which figures 9a and 9b are extracted. For these calculations a full potential non viscous code (FP3D) developed at the ONERA has been used. Figure 9a shows an excellent agreement between theory and experiment at the blade tip.

5.2. Pressure measurements on inboard sections

Figures 7 and 8 show no shocks on the profile's upper surface for sections $r/R_1 = 0.700$ and $r/R_1 = 0.500$. At 0° azimuth angle and for the section at $r/R_1 = 0.500$ the pressure curve is very flat and this is still rather true at 30° azimuth. This can be caused by a fluid velocity that remains high, that is to say that there is no recompression. This is normally the case for stalled profiles but here the lift and hence the angles of attack (figure 2) are very small. On the lower surface, the pressure behaves as would be expected on a subsonic upper surface: this is not too astonishing if the angle of attack is very small. It is the difference between the upper and the lower surfaces that generates the nose down moment.

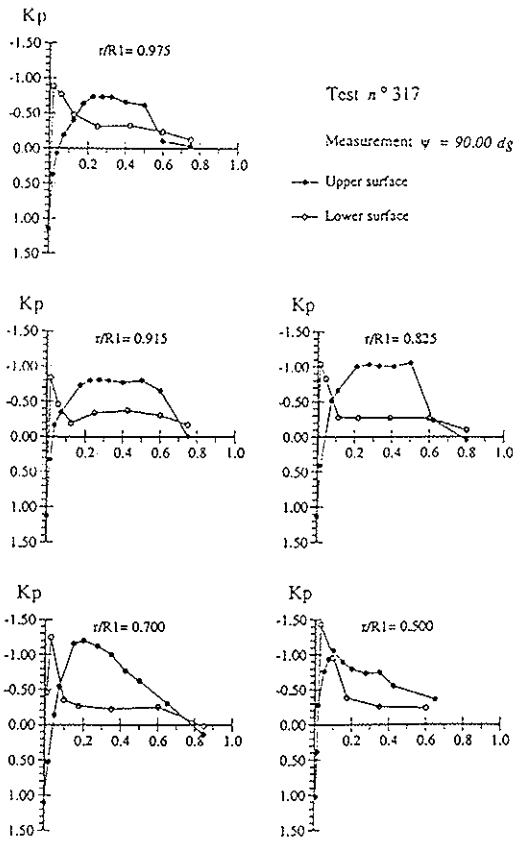

Figure 8. Measured pressure distributions for test case n°317 at 90° azimuth angle

For the section at $r/R_1 = 0.700$ things are not so clear, the upper surface has a pressure distribution which is intermediate between the distribution of the section at $r/R_1 = 0.500$ and one which is characteristic of the tip sections. At 90° azimuth the same comments as above can be made. This suggest that on the advancing side of the rotor disc, separation or some other viscous effect of the same kind is at work. This phenomenon could possibly be a consequence of the large variations in the profile normal velocity. This explanation is supported by the full potential calculation of figure 9b which shows that the FP3D code fails to predict the strong nose down moments experienced by the blade's inboard most section.

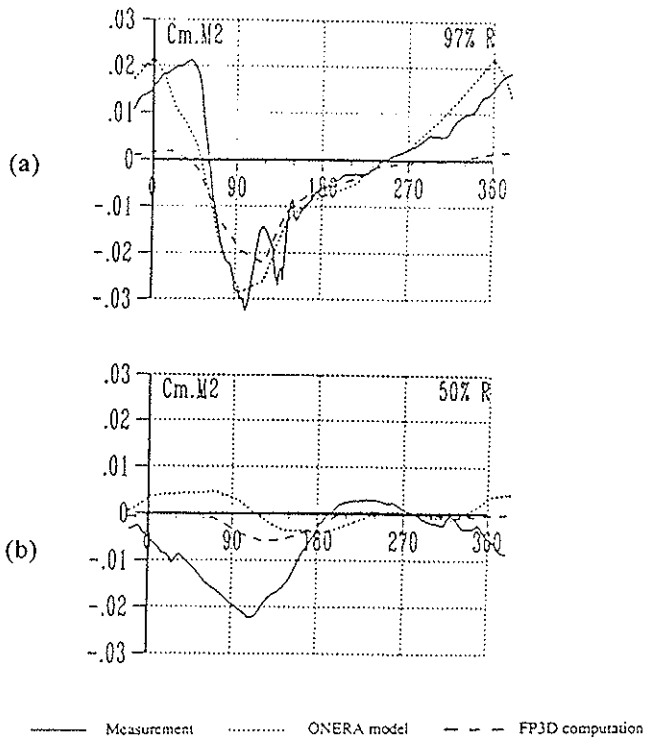

Figure 9. Moments for test case n°337 (taken from [4] and [7])

6. Application to aeroelastic computation

The correction added to the standard ONERA model for aerodynamic moments has been tailored to give the best possible results when the angle of attack, the velocity and the sweep angle are all given as functions of the time. One question remains to be answered, how does the extended model perform when introduced into a complete aeroelastic code such as "ROTOR" [4] ? The coupling between the blade torsion and the aerodynamic moments may generate numerical instabilities. This happens when models are applied with conditions which are outside the original range for which the parameters are defined. It could be the case here for blade sections closer to the root than the closest instrumented section ($r/R_1 = 0.500$) or for any section of the blade on the retreating side of the rotor disc (azimuth > 180°).

The correction developed in this paper has been applied to a wide range of flight conditions and no such numerical instabilities have occurred. Results for test cases 317, 337 and 358 at advance ratios of 0.4, 0.45 and 0.50 are presented. The blade dynamics is modeled by its first 7 non rotating natural modes. The induced velocity on the rotor disc is given by METAR which is a lifting line code, developed by Eurocopter France [4, 7], using incompressible vortex filaments with corrections for compressibility.

The calculations were carried out under the following conditions:

- 4 control setting parameters:
  - the inclination of the rotor hub (1 parameter)
  - the collective and cyclic pitch (3 parameters).
- These parameters were adjusted so as to satisfy 4 conditions:
  - to obtain the measured rotor lift,
  - to obtain the measured rotor advancing force,
  - zero lateral tilt angle ($\beta_s = 0$)
  - longitudinal rotor tilt equal to the sine component of the cyclic pitch angle.

The last two conditions constitute a wind tunnel control law known as the "Modane law". This arbitrary control law was applied for all the test cases dealt with here. The measured loads are used as the test condition references in order to minimise the uncertainties occurring in parameter measurements and in the control angle settings during the tests.

6.1. Results for test 317 at an advance ratio $\mu = 0.40$

The results of the computations for case 317 show some improvements for the lift forces on the instrumented sections. The results for the moments are shown in figure 10. As expected, the nose up moment at the blade tip (-60° to +30° azimuth angles) is now well predicted and this is also the case for the nose down moment at the inboard sections around the 90° azimuth. For the blade tip, the complex behaviour of the moment curve around the 90° azimuth is not obtained with all its details in spite of the modelling discussed in 4.3.1 and 4.3.2.

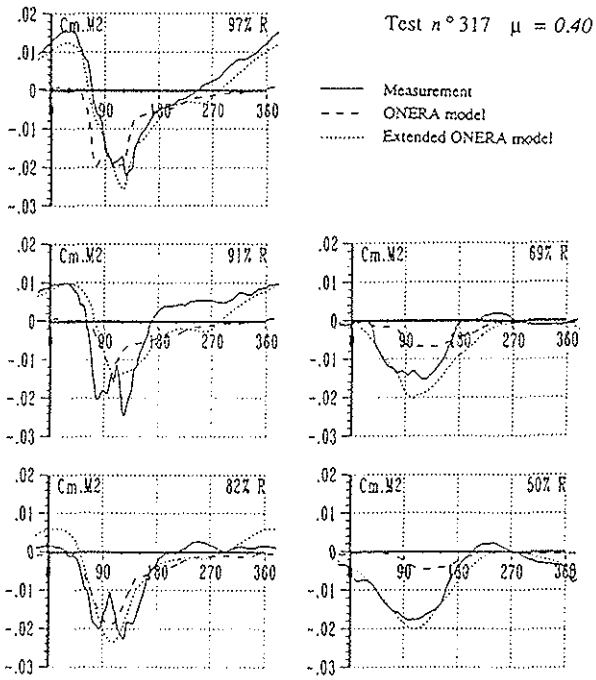

Figure 10. Measured and calculated moments for test n°317

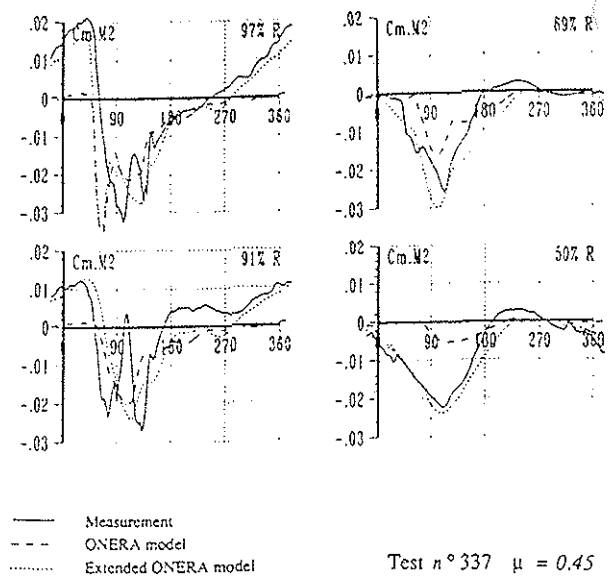

Figure 11. Measured and calculated moments for test n°337

6.2. Results for test 337 at an advance ratio $\mu = 0.45$

The same comments can be made here as for test 317. The results for the moments are given in figure 11. The comparison between the experimental and theoretical blade torsion at the blade tip is shown in figure 12. Though the results are closer to the measurements, it must be stressed that firstly, there is some uncertainty in the measurement of the steady part of the torsional angle, and secondly, the amplitudes of the high harmonic components of the torsional angle are not accurately predicted. A better modelling of the aerodynamic forces such as that using Hopf's bifurcation [9, 10] may improve correlation.

6.3. Results for test 358 at an advance ratio $\mu = 0.50$

For this test, the measurements are available only on the two blade sections closest to the tip (figure 13). Here the correction has limited effects on the predicted moments. The very large nose down moment experienced by the blade tip sections between 60° and 150° azimuth angles is not predicted correctly. This clearly shows the limitation of the method. This problem was also apparent when the angle of attack was an input parameter. It may in part be due to the fact that the high advance ratio tests were outnumbered in the modelling by cases with more moderate values of μ. This results in less weight being given to high advance ratio cases in optimising the error function.

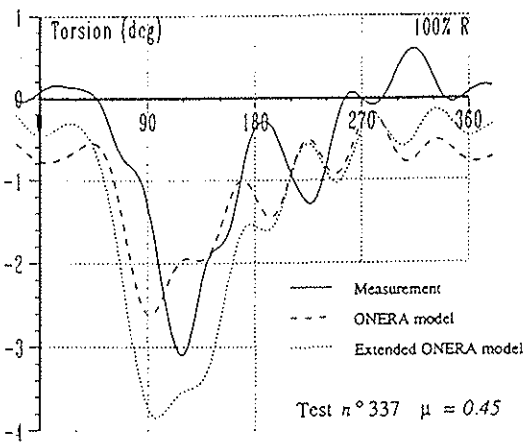

Figure 12. Measured and calculated torsion at the blade tip

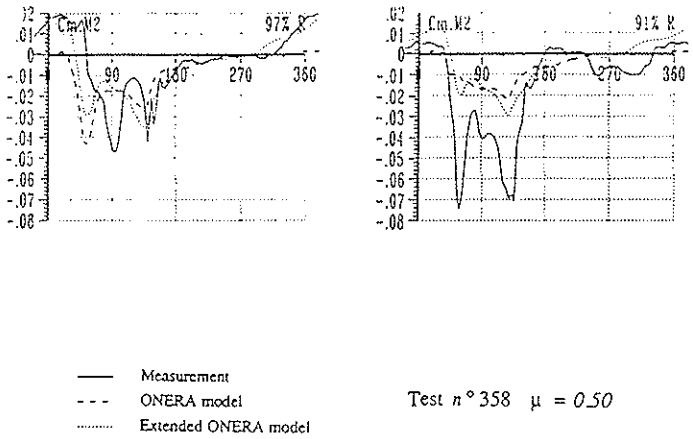

Figure 13. Measured and calculated moments for test n°358

7. Conclusions

Predictions of the aerodynamic forces on a rotor by means of the "ROTOR" code, which uses a standard model of the 2D forces based on linear differential equations, fails to predict the nose up moment at the blade tip and the nose down moment on inboard sections of the blade. The analysis of experimental data and comparison with results given by a non viscous CFD code suggest two distinct reasons for this weakness of the model. At the blade tip unsteady transonic effects seem to explain the observed moments over the full range of azimuth angles. Here the phenomena seem non viscous and the rate of change of the angle of sweep is possibly not a very important factor. On more inboard sections around the 90° azimuth angle, some flow separation seems to occur even for small angles of attack and may be induced by the unsteady conditions of the flow (velocity, sweep).

The standard model has been extended through a corrective term introduced by means of a linear differential equation with a non linear forcing function. A discrete-time version of this extension has been integrated into the full aeroelastic "ROTOR" code. Comparisons between calculations and measurements on a rotor show significant improvements to predicted moments for advance ratios up to 0.45.

Acknowledgments

The author wishes to thank Eurocopter France for the authorization to publish the experimental data and the French Ministry of Defence (DRET-6) for supporting this study.

References

[1] Maier T.H. and Bousman W.G. *An examination of the aerodynamic moment on rotor blade tips using flight test data and analysis.* 18th European Rotorcraft Forum, Avignon, France, 1992.

[2] Petot D. *Modélisation du décrochage dynamique par équations différentielles.* La Recherche Aérospatiale, n° 5-1989, pp. 59 to 72, 1989.

[3] Costes J-J. and Petot D. *Forces aérodynamiques couplées dues au décrochage instationnaire sur une aile de grand allongement oscillant à grande amplitude.* AGARD/SMP Sorrento, Italy, 1990.

[4] Bessone J. and Petot D. *Calculs du comportement aéroélastique des rotors comparés à l'expérience.* La Recherche Aérospatiale, n°1-1995, pp. 3-14, 1995.

[5] Tourjansky N. and Széchényi E. *The measurement of blade deflections. A new implementation of the strain pattern analysis.* 13th European Rotorcraft Forum, Avignon, France, 1992.

[6] Greenberg J.M. *Airfoil in sinusoidal motion in a pulsating stream.* Nasa Technical note n° 1326, 1947.

[7] Petot D. and Allongue M. *Aéroélasticité des rotors d'hélicoptères. Synthèse des travaux et perspectives.* Revue Française de Mécanique n°1995-1, 1995.

[8] Press W.H., Flannery B.P., Teukolsky S.A. and Vetterling W.T. *Numerical recipes. The art of scientific computing.* Cambridge University Press, 1989.

[9] Truong V.K. *A 2-D dynamic stall model based on a Hopf bifurcation.* 19th European Rotorcraft Forum, Cernobbio, Como, Italy, 1993.

[10] Truong V.K. *Prévision des charges sur une pale d'hélicoptère basées sur le modèle de bifurcation de Hopf.* 31ème Colloque d'Aérodynamique Appliquée (AAAF), Paris, France, 1995.